

Revista Mexicana de Astronomía y Astrofísica

Revista Mexicana de Astronomía y Astrofísica
Universidad Nacional Autónoma de México
rmaa@astroscu.unam.mx
ISSN (Versión impresa): 0185-1101
MÉXICO

2002

T. I. Larsen / J. Sommer Larsen / B. E. J. Pagel
THE CHEMICAL EVOLUTION OF GAS-RICH DWARF GALAXIES
Revista Mexicana de Astronomía y Astrofísica, volumen 012
Universidad Nacional Autónoma de México
Distrito Federal, México
pp. 201-206

Red de Revistas Científicas de América Latina y el Caribe, España y Portugal

Universidad Autónoma del Estado de México

reDalyC
LA BIBLIOTECA CIENTÍFICA EN LÍNEA
<http://redalyc.uaemex.mx>

THE CHEMICAL EVOLUTION OF GAS-RICH DWARF GALAXIES

T. I. Larsen,¹ J. Sommer-Larsen,² and B. E. J. Pagel³

RESUMEN

En un esfuerzo por entender la evolución de las abundancias de N, O y He en galaxias enanas ricas en gas, investigamos la difusión y mezclado de eyectas de supernovas en relación con la evolución de regiones H II y desarrollamos un modelo numérico de evolución química basado en un modo de doble brote de formación estelar (con un intervalo del orden de 3×10^7 años entre brotes de un par), el cual toma en consideración la existencia de una dispersión significativa en la relación entre N/O y O/H. Se explora la dependencia de las abundancias en la fracción de gas de estos modelos y modelos similares, en combinación con varias hipótesis concernientes a la inyección y expulsión de gas selectiva y no selectiva. Las fracciones de gas son inciertas dentro de amplios límites para galaxias compactas azules, pero están mejor definidas para algunas enanas irregulares. Se encuentra que los vientos selectivos no dan un buen ajuste a N/O, mientras que los modelos cerrados y modelos con vientos no selectivos con o sin acreción son todos viables.

ABSTRACT

In an effort to understand the evolution of N, O, and He abundances in gas-rich dwarf galaxies, we investigate the dispersion and mixing of supernova ejecta in relation to H II region evolution and develop a numerical model of chemical evolution based on a double-bursting mode of star formation (with an interval of the order of 3×10^7 years between bursts of a pair) which has been designed to account for the existence of significant scatter in the N/O–O/H relation. The dependence of the abundances on gas fraction is explored on the basis of this and similar models, in combination with various hypotheses concerning inflow and selective and non-selective outflow. The gas fractions are uncertain within wide limits for blue compact galaxies, but more well defined for some dwarf irregulars. Selective winds do not give a good fit to N/O, while closed models and models with non-selective winds with or without inflow are all found to be viable.

Key Words: **GALAXIES: ABUNDANCES — GALAXIES: IRREGULAR — GALAXIES: STARBURST — H II REGIONS**

1. INTRODUCTION

The chemical evolution of dwarf irregular (dIrr) and blue compact emission-line galaxies (BCGs) is of particular interest because a substantial body of observational data is available and some degree of simplicity exists because of the low level of “metal” enrichment and the absence of large abundance gradients. Furthermore, their wide range of intrinsic properties makes them suitable objects for testing certain expectations from stellar nucleosynthesis theory and the “simple” or other models of galactic chemical evolution, although at the same time there are complications associated with the inflow of unprocessed material, outflow in homogeneous or selective galactic winds and bursting (or “gasping”) modes of star formation. Chemical evolution models attempt to apply all these concepts to account for the distribution of different elements, notably helium, oxy-

gen and nitrogen, in relation to star formation rates and gas fractions. Because many parameters such as these last two are generally very poorly determined, the most convincing tests come from the comparison of different elements with one another.

In this paper we address a number of issues that have been raised in connection with these objects: Self-enrichment and the origin of scattering in the N/O relation; the relation between chemical composition and gas fraction; and the influence of homogeneous or metal-enhanced outflow. A more complete version of this work can be found in Larsen, Sommer-Larsen, & Pagel (2001).

2. THE SAMPLE

Figure 1 shows N/O ratios for the selected sample of galaxies. With the possible exception of the DLA systems, they show a constant level for $12 + \log(\text{O}/\text{H}) < 8$, implying that the major part of the nitrogen is produced as a primary element. For $12 + \log(\text{O}/\text{H})$ above about 8, N/O is an increasing function of metallicity, suggesting the major part of

¹Copenhagen University Observatory, Denmark.

²Theoretical Astrophysics Center, Copenhagen, Denmark.

³Astronomy Centre, Sussex University, UK.

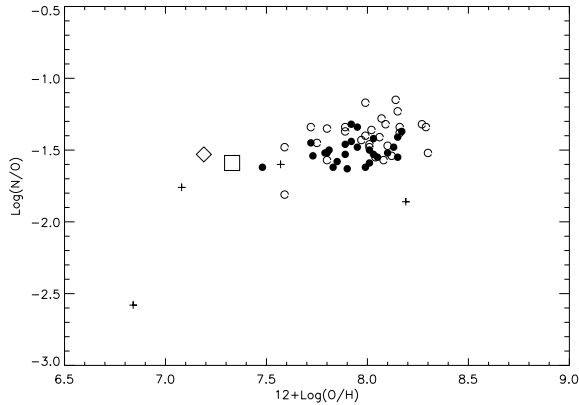


Fig. 1. The sample of observations used in this paper. The symbols are: diamond=I Zw 18 (Izotov & Thuan 1998); square=SBS 0335-052 (Izotov et al. 1997b), filled circles are BCGs (Izotov et al. 1997a) and open circles are BCGs and dIrrs (Pagel et al. 1992). Finally, the plus symbols are DLA systems (Lu, Sargent, & Barlow 1998).

the nitrogen to be secondary. These trends are well known, see e.g., Garnett (1990), Vila-Costas & Edmunds (1993), Pettini, Lipman, & Hunstead (1995), van Zee, Salzer, & Haynes (1998a) and Henry, Edmunds, & Köppen (2000).

Furthermore, the scatter in N/O seems to be significant and our models are based on this assumption. If we fit a straight line to our selected observations, ignoring the DLAs, we find the standard deviation in N/O to be $\sigma = 0.11$ dex, which is of the same order of magnitude as the observational uncertainty (Izotov et al. 1997a), but a real scatter is evident in other data from a wider range of sources, see e.g., Kobulnicky & Skillman (1996).

The DLA systems pose severe problems when observing N and O abundances. Usually the N-lines appear on top of underlying absorption, and O-lines are almost always saturated. Because of these difficulties, Lu et al. (1998) found it useful to use Si or S instead of O, which makes sense as O/Si and O/S are found to be the same as solar in both the Galactic disc and halo as well as H II regions in nearby galaxies. The question is whether the abundance ratios are equal to solar at the extreme low metallicity of DLAs. This is by now the largest uncertainty in this method. Thus, in Figure 1, the DLAs are represented by their N/Si and Si/H, assuming that these ratios are equivalent to N/O and O/H. Four systems have been selected from the Lu et al. sample. For the rest of their sample, the quality of the observations permits only upper or lower limits to abundances to be derived.

3. EJECTA DISPERSAL AND MIXING

Many chemical evolution models assume a one-zone description with instantaneous mixing. Assigning the term one-zone to a BCG seems to be quite a poor approximation, and assuming the mixing to be instantaneous will always be doubtful. However, if we choose to reject these assumptions, we are faced with the problem that no complete theory of mixing is available at present. The problem is that the gas dynamics following a starburst are very complex. The energy input into the ISM comes from photoionization and stellar winds from massive stars followed by SN type II. Different scenarios have been proposed for the dispersal and mixing processes. One of the propositions has been ‘self-enrichment’, referring to the suggestion that only the H II region surrounding the newly formed star cluster is enriched with heavier elements, in particular oxygen. Thus, the observed abundances, using emission lines, may be considerably higher than they would be if observed in the neutral medium. The idea was originally proposed by Kunth & Sargent (1986), suggesting that the enrichment is confined to take place within the Strömgren sphere. However, the hypothesis is controversial, and a lot of opposing arguments exist. Use of self-enrichment implies the assumption of almost instantaneous mixing within H II regions. The problem is that the correlated energy input of SNe changes the physical conditions of H II regions dramatically. In fact, the density is decreased by a factor 10^3 – 10^6 and the temperature increased by a similar factor behind the SN-driven shock front. The observed lines of singly or doubly ionized N and O cannot arise from such extreme conditions. A future project could be X-ray abundance observations. If the observed emission lines cannot form within the superbubble/supershell (hereinafter a ‘superbubble’ is a wind-driven bubble, while a ‘supershell’ is a SN-driven shell), they may arise from a region outside the shock front. But according to detailed numerical hydrodynamical models (Tenorio-Tagle 1996), the ejecta will stay within the superbubble/supershell for a large part of their evolution, not enriching the surrounding medium. To test the viability of this statement, a few calculations are presented below, comparing radii of superbubbles/supershells and radii of H II regions. Furthermore, observations give evidence against the self-enrichment hypothesis, see e.g., van Zee et al. (1998b), Kobulnicky & Skillman (1998).

3.1. H II Region Evolution

In the following, the radii of H II regions are calculated for comparison with superbubble/supershell

radii, assuming the H II region to be a Strömgen sphere within which all ionizing photons are absorbed. Spitzer (1978) gave the following relation for the radius R of the H II region as a function of time t :

$$R(t) = R_0 \left(1 + \frac{7 C_{\text{II}} t}{4 R_0} \right)^{4/7}, \quad (1)$$

where C_{II} is the sound speed in the H II region, assuming that the expansion velocity nearly equals that of the associated shock. However, this assumes a constant flux N of ionizing photons, which is unrealistic for an instantaneous starburst, so we replace equation (1) by

$$\left[\left(\frac{N_0 R^3}{N R_0^3} \right)^{1/2} - \frac{1}{4} \right] \left(\frac{dR}{dt} \right)^2 - \frac{dN/dt}{6\beta R^2 \rho_{\text{II}}^2} \left(\frac{dR}{dt} \right) - \left(\frac{dN/dt}{6\beta R^2 \rho_{\text{II}}^2} + \frac{C_{\text{II}}^2}{\gamma} \right) = 0, \quad (2)$$

where β is a combination of atomic constants, which is solved for dR/dt leading to a differential equation that is then solved numerically taking the photon flux from Stasińska & Leitherer (1996).

The newly formed star cluster begins after 3 Myr or so to expel matter in form of a superbubble, succeeded shortly afterwards by a supernova-driven supershell, the radius of which is calculated from an analytic formula by McCray & Kafatos (1987)

$$R_s = 97 (N_* E_{51} / n_e)^{1/5} t_7^{3/5} \text{ pc}, \quad (3)$$

where N_* is the number of stars with mass above $8 M_{\odot}$ in the cluster, and t_7 the time in units of 10 Myr. Assuming an instantaneously formed cluster of $10^6 M_{\odot}$ with a Salpeter IMF from 0.1 to $100 M_{\odot}$ with initial electron density $n_e = 10 \text{ cm}^{-3}$ and uniform expansion, it turns out that, for the first 6 Myr—i.e., virtually throughout the period of visibility of the H II region—the H II radius (250 pc after 6 Myr) appreciably exceeds that of the supershell, reinforcing the conclusion that the H II region spectrum is unlikely to be affected by self-enrichment from its own starburst.

3.2. Propagating Star Formation

Propagating star formation means that the energy deposited in the ISM by an evolving star formation event initiates new star formation. As a supershell grows, it becomes Rayleigh-Taylor unstable and fragments. The situation has been treated by Elmegreen (1994), who found an expression for the

timescale of cloud-collapse in the supershell

$$t_{\text{cloud}} = 103 \left(\frac{n_0 \mathcal{M}}{\text{cm}^{-3}} \right)^{-1/2} \text{ Myr}, \quad (4)$$

where \mathcal{M} is the expansion speed of the shell divided by the rms velocity dispersion in the shell. For an adiabatic shell, $\mathcal{M} = 1.8$ (Elmegreen 1994). If $n_0 = 10 \text{ cm}^{-3}$, this gives the result that star formation is expected to start not earlier than ~ 24 Myr after shell formation. On the other hand, if $n_0 = 3 \text{ cm}^{-3}$ as used in the calculations above for a typical density in the late stages of H II-region evolution, the timescale is more like 44 Myr. The mass of the supershell is given as

$$M = \rho_0 V_{\text{ss}} \approx 1.3 n_0 m_p \frac{4\pi}{3} R^3, \quad (5)$$

assuming all of the ISM originally within R to be incorporated in the shell. ρ_0 is the mass density of the ambient medium, V_{ss} is the volume occupied by the hot phase within the supershell, m_p is the proton mass and 1.3 is the approximate mass per particle in units of the proton mass. The radius is of order a few 100 pc as shown above, so equation (5) gives a shell mass of the order $10^6 M_{\odot}$. Hence the induced star formation is of the same order of magnitude as the original central burst, but well separated in time.

If the ejected metals from the central burst mix with the material of the supershell, the H II regions of the induced burst will show different abundances from the central H II region. Although there has been some doubt as to whether the metals are allowed to mix into the supershell (Tenorio-Tagle 1996), and—if so—when this will happen, we have been inspired by this possibility to let our model have a double burst nature.

4. THE MODEL

We have designed a model to fulfill certain demands, namely that the observed trend of constant N/O for low metallicities and increasing N/O for higher metallicities should be reproduced and also that the observed scatter in N/O should be explained. Fixing all the parameters by fitting the N/O-O/H evolution, the model should also be able to explain the observed helium mass fraction as a function of O/H and O/H as a function of gas fraction.

The included elements are H, He, C, N, and O. The production of N is still a hot topic, since the degree of primary production at various metallicities is unclear. Further, N is produced mainly by intermediate mass stars while O is produced by massive

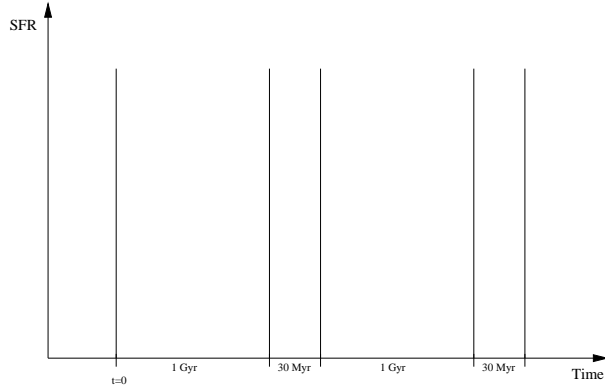


Fig. 2. Schematic of burst sequence in our model.

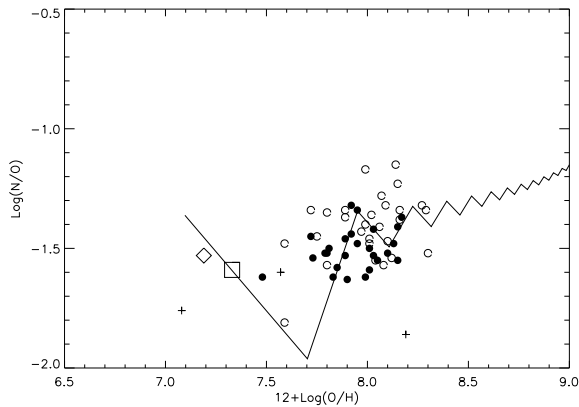


Fig. 3. Evolution of N/O ratio using yield set 2b, a lower mass limit of $0.01 M_{\odot}$ to the Salpeter IMF, a first burst of $2 \times 10^6 M_{\odot}$, subsequent bursts of $6 \times 10^6 M_{\odot}$, $\alpha = 1.1$ and the upper limit for hot bottom burning is $5 M_{\odot}$.

stars, making it necessary to include stellar lifetimes. However, the inclusion of both N and O provides the opportunity of constraining stellar parameters and mixing scenarios.

To account for the scatter in N/O, it is suggested that the bursts are instantaneous and ordered in pairs, hence using the delay between the ejection of N and O. The principle of time delay was used by Garnett (1990), though employing single bursts only. It is doubtful whether single bursts produce scatter, since at least some abundance observations have to be done at the time of N-release. However, this is between two bursts, where no giant H II-regions are present, providing no possibility for abundance observations using emission lines. Double bursts produce the scatter quite naturally: It was found reasonable above that a localized burst results in another burst, this time in the expanding supershell, surrounding the original burst. The

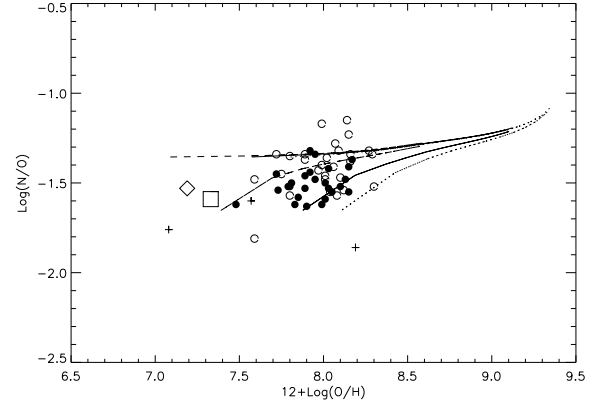


Fig. 4. Upper and lower bounds to N/O ratio using yield set 3. Dashed lines correspond to burst masses equal to 1 per cent of the total mass of the dwarf galaxy, solid lines to 3 per cent and dash-dotted lines to 5 per cent. For these runs, all primary yields have been extrapolated for metallicities lower than the range covered by the yield sources.

timescale for star formation in the supershell is found to be $\gtrsim 2.4 \times 10^7$ yr, comparable to the timescale for O-ejection, but shorter than the timescale for N-ejection (50 to 150 Myr), hence producing the desired scatter.

In our model, we assume that the very first burst is a single one, all the others appearing in pairs (see Fig. 2). The inter-burst period within a pair is tuned to give maximum scatter in N/O, which turns out to be 30 Myr. The time between pairs is set arbitrarily to 1 Gyr; this value could be anything above about 100 Myr.

We calculate numerically the abundances of each of the above-mentioned elements and the gas fraction after each burst using the Salpeter IMF and four sets of theoretical yields:

- Set 1. Massive stars: Maeder (1992; large mass loss) and Woosley & Weaver (1995). Intermediate-mass stars: van den Hoek & Groenewegen (1997). Metallicities $Z = 0.001$ to 0.02 .
- Set 2a. Massive stars: as in Set 1. Intermediate-mass stars: Renzini & Voli (1981).
- Set 2b. As for 2a, but with lower mass loss above $9 M_{\odot}$.
- Set 3. Massive stars: Portinari et al. (1998); metallicities 0.0004 to 0.02 . Intermediate and low-mass stars: Marigo et al. (1996; 1998); metallicities 0.008 to 0.02 .

Models have been computed with or without mass loss accompanying the stellar bursts in metal-enhanced or homogeneous winds (cf. Pilyugin 1993),

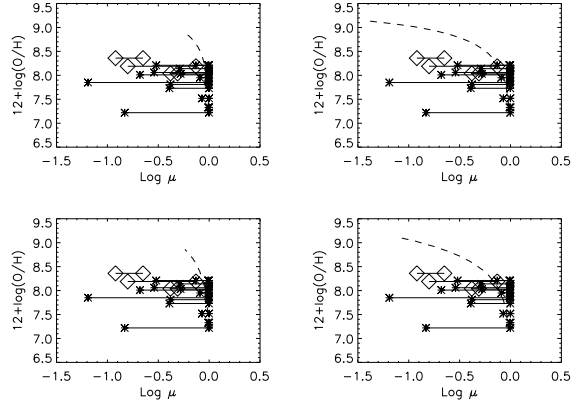


Fig. 5. Oxygen abundance as a function of gas fraction μ in closed models. Top plots are for set 2a, for $M_{\text{low}} = 0.1 M_{\odot}$ to the left and $0.01 M_{\odot}$ to the right. Bottom plots are the same for set 3. Dashed lines are outputs from the models for burst masses of $2 \times 10^6 M_{\odot}$ to the left and $4 \times 10^6 M_{\odot}$ to the right, both for a total galaxy (star + gas) mass of $10^8 M_{\odot}$. Asterisks represent lower and upper limits estimated from observational data for BCGs, the lower limit from dynamical arguments and the upper one from assumed mass: light ratios for a young starburst. Diamonds represent the LMC, NGC 6822 and the SMC, for which better upper limits can be estimated from a mass: light ratio based on the star formation history.

and some models have also included inflow of unprocessed material.

5. RESULTS

5.1. N/O Ratios

Some results (for closed models) are shown in Figures 3 and 4. The various burst masses assumed seem to cover the observed dispersion fairly well. At the higher metallicities, our models fit the lower envelope of N/O abundances reported, e.g., by Van Zee et al. (1998a), giving about 1/3 of solar N/O at $12 + \log(\text{O}/\text{H}) = 8.8$; higher ratios are accounted for in the models by Henry et al. (2000).

5.2. Gas Fractions: Effects of Winds

Figure 5 shows the predicted relation between oxygen abundance and gas fraction for our closed models, compared with some observational data, and displays the well known discrepancy between theoretical and empirical yields based on such models.

This discrepancy can be cured using selective winds (Fig. 6, top panel), but at the expense of an unacceptably high N/O ratio (middle panel). (The helium-oxygen relation is less affected—lower panel.) Ordinary (non-selective) winds leave the N/O, O/H

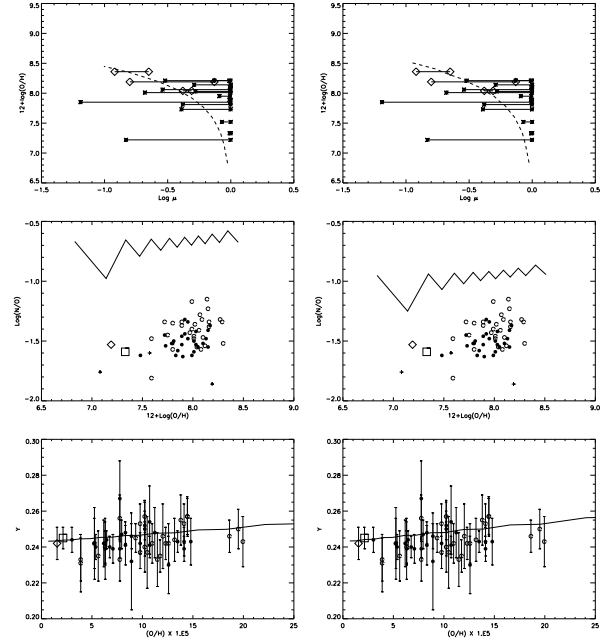


Fig. 6. Results of models with metal-enhanced winds using yield set 2a, burst mass $6 \times 10^6 M_{\odot}$ and wind efficiency 0.8 (on the left), and yield set 3 with wind efficiency 0.7 (on the right). The bottom panels show the Y, O/H relations.

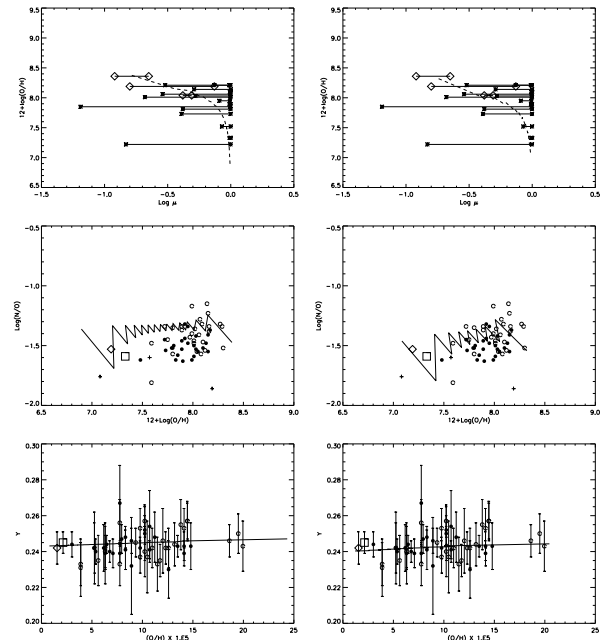


Fig. 7. Results of models combining inflow on a 5 Gyr time-scale with homogeneous outflow. Left, yield set 2a, with wind efficiency 8, burst mass $3 \times 10^6 M_{\odot}$, inflow constant $8 \times 10^8 M_{\odot}$. Right, yield set 3, wind efficiency 5, burst mass $6 \times 10^6 M_{\odot}$, inflow constant $7 \times 10^8 M_{\odot}$.

relation more or less intact, but still have problems fitting the details of the relation with gas fraction. Addition of inflow (Fig. 7) permits all the constraints to be honored, at the expense of a multiplicity of parameters.

This work was supported by Danmarks Grundforskningsfond through its support for the Theoretical Astrophysics Center.

REFERENCES

- Elmegreen, B. G. 1994, *ApJ*, 427, 384
 Garnett, D. R. 1990, *ApJ*, 363, 142
 Henry, R. B. C., Edmunds, M. G., & Köppen, J. 2000, *ApJ*, 541, 660
 Izotov, Y. I., Lipovetsky, V. A., Chaffee, F. H., Foltz, C. B., Guseva, N. G., & Kniazev, A. Y. 1997b, *ApJ*, 476, 698
 Izotov, Y. I., & Thuan T. X. 1998, *ApJ*, 497, 22
 Izotov, Y. I., Thuan, T. X., & Lipovetsky V. A. 1997a, *ApJS*, 108, 1
 Kobulnicky, H. A., & Skillman, E. D. 1996, *ApJ*, 471, 211
 ———. 1998, *ApJ*, 497, 601
 Kunth, D., & Sargent, W. L. W. 1986, *ApJ*, 300, 496
 Larsen, T. I., Sommer-Larsen, J., & Pagel, B. E. J. 2001, *MNRAS*, 323, 555
 Lu, L., Sargent, W. L. W., & Barlow, T. A. 1998, *AJ*, 115, 55
 McCray, R., & Kafatos, M. 1987, *ApJ*, 317, 190
 Maeder, A. 1992, *A&A*, 264, 105
 Marigo, P., Bressan, A., & Chiosi, C. 1996, *A&A*, 313, 545
 ———. 1998, *A&A*, 331, 564
 Pagel, B. E. J., Simonson, E. A., Terlevich, R. J., & Edmunds, M. G. 1992, *MNRAS*, 255, 325
 Pettini, M., Lipman, K., & Hunstead, R. W. 1995, *ApJ*, 451, 100
 Pilyugin, L. S. 1993, *A&A*, 277, 42
 Portinari, L., Chiosi, C., & Bressan, A. 1998, *A&A*, 334, 505
 Renzini, A., & Voli, M. 1981, *A&A*, 94, 175
 Spitzer, L. Jr. 1978, *Physical Processes in the Interstellar Medium* (Dordrecht: Wiley)
 Stasińska, G. & Leitherer, C. 1996, *ApJS*, 107, 661
 Tenorio-Tagle, G. 1996, *AJ*, 111, 1641
 van den Hoek, L. B., & Groenewegen, M. A. T. 1997, *A&AS*, 123, 305
 van Zee, L., Salzer, J. J., & Haynes, M. P. 1998a, *ApJ*, 497, L1
 van Zee, L., Westpfahl, D., & Haynes, M. P. 1998b, *AJ*, 115, 1000
 Vila-Costas, M. B., & Edmunds, M. G. 1993, *MNRAS*, 265, 199
 Woosley, S. E., & Weaver, T. A. 1995, *A&AS*, 101, 181



Miriam Peña and Bernard Pagel

- T. I. Larsen: Copenhagen University Observatory, Juliane Maries Vej 30, DK-2100 Copenhagen Ø, Denmark (thommy_l@astro.ku.dk).
 J. Sommer-Larsen, Theoretical Astrophysics Center, Juliane Maries Vej 30, DK-2100 Copenhagen Ø, Denmark (jslarsen@tac.dk).
 B. E. J. Pagel, Astronomy Centre, CPES, University of Sussex, Brighton BN1 9QJ, UK (bejp@star.cpes.susx.ac.uk).